

TLS AND UAV PHOTOGRAMMETRY FOR THE USE OF HERITAGE BUILDING INFORMATION MODELLING DEVELOPMENT: A CASE STUDY OF THE SARAWAK ISLAMIC HERITAGE MUSEUM

CHANG SAAR CHAI^{1,2}, YAOLI XIONG^{1,*}, AMMAR NAZAR HANIFA³,
SYAHRIR IMAN SUIB⁴, SOON LAM TATT¹

¹School of Architecture, Building and Design, Taylor's University, Taylor's Lakeside
Campus, No. 1 Jalan Taylor's, 47500, Subang Jaya, Selangor DE, Malaysia

²UTM Construction Research Center (UTM CRC), Univeristi
Teknologi Malaysia, Jalan Iman, 81310 Skudai, Johor, Malaysia

³Faculty of Engineering, Computing and Science, Swinburne University of Technology
Sarawak Campus, Jalan Simpang Tiga, 93350 Kuching, Sarawak, Malaysia

⁴EPR Sdn Bhd, Malaysia

*Corresponding Author: 0370032@sd.taylors.edu.my

Abstract

The 3D archiving and documentation of cultural heritage have been gaining importance. As-built HBIM (Heritage Building Information Modelling) aids in preserving key characteristics that are crucial for restoration following man-made or natural damage. The accuracy of these models largely depends on data acquisition methods, with Terrestrial Laser Scanning (TLS) and Unmanned Aerial Vehicle (UAV) photogrammetry being the most commonly used. However, this integration has some limitations due to the constraints in fixing the relative positions between the two data sets. This study examines the integration of TLS and UAV photogrammetry to produce accurate HBIM models for heritage sites. A case study was conducted at the Sarawak Islamic Heritage Museum in Malaysia, where data was captured using Ground Control Points (GCP) and Global Positioning System (GPS) coordinates. The resulting point clouds were processed, integrated, and imported into Revit for family creation and HBIM modelling. Both integration techniques yielded point clouds with errors within the tolerance levels specified by the Sarawak Building Ordinance 1994. While the GCP method produced more accurate results, GPS offered faster data acquisition, eliminating the need for additional GCP surveys. Both methods show potential for creating reliable HBIM models for heritage conservation.

Keywords: Ground control points (GCP), Global positioning system (GPS), Heritage building information modelling (HBIM), Terrestrial laser scanning (TLS), Unmanned aerial vehicle (UAV).

The term "heritage building information modelling" (HBIM) appears in a separate but interconnected cluster, linked to concepts like "digital twin," "digital heritage," and "parametric objects." This cluster reflects the evolution of heritage modelling beyond traditional documentation towards dynamic and intelligent systems that support conservation and management. Related terms such as "infrared thermography" and "machine learning" suggest the growing incorporation of advanced technologies for analysis and interpretation in HBIM workflows.

However, the VOSviewer analysis reveals a critical research gap in integrating terrestrial laser scanning (TLS) and UAV photogrammetry into heritage building information modelling (HBIM). While these technologies are widely used for spatial data collection, their combined application within unified HBIM workflows remains underexplored. Strong links between "TLS," "UAV photogrammetry," and "3D reconstruction" highlight their importance. Still, weaker connections to "HBIM" and terms like "digital twin" and "parametric objects" suggest a lack of standardised processes for converting raw data into intelligent models.

Emerging technologies, such as "machine learning" and "infrared thermography," show potential to address data fusion and automation challenges but are underutilised. These limitations underscore the need for robust workflows to enhance HBIM's role in heritage preservation. Addressing this gap could advance modelling accuracy and efficiency, enabling more effective heritage building management. Optimising the integration of terrestrial laser scanning (TLS) and UAV photogrammetry workflows to address the current limitations of Heritage Building Information Modeling (HBIM). This provides a solid foundation for investigating innovative solutions to existing challenges.

Moreover, studies have been conducted to investigate the applicability of TLS and UAV photogrammetry for generating HBIM models. These studies mainly focus on using one technology to generate models, with limited research being conducted on integrating the two technologies to generate the HBIM model. The following section describes the past research conducted.

The application of UAV photogrammetry with desktop studies and traditional surveying techniques to generate 3D HBIM models was investigated by Karachaliou in 2019 for preventive actions for cultural heritage sites. UAV photogrammetry was used to capture data from locations that were difficult to access. The data from UAV photogrammetry was augmented with a desktop study and traditional surveys to produce a complete and accurate HBIM model.

However, the limitations of this technique are the long and tedious process of the desktop study and traditional survey and image distortions due to image viewing angles. The accuracy and speed of this technique can be improved with the use of TLS to hasten the conventional surveying methods, as suggested by Karachaliou et al. [4]. Integrating the TLS and UAV photogrammetry data should also improve the accuracy of the generated model. Additional limitations include the inability of UAV photogrammetry to capture data from interior surfaces. This limitation can be eliminated using TLS, as highlighted by Karachaliou et al. [4].

TLS was also investigated by Baik et al. in 2021 [6]. The paper studied the application of TLS with desktop studies for the architectural documentation and surveying of heritage sites to generate inventories of heritage buildings. TLS was chosen for its rapid data capture abilities and the accuracy of data produced. To

produce a complete 3D model, a desktop study was conducted to find missing information. Again, it was highlighted that the limitation of this study was the long and tedious desk study to find missing information. As well as the inability of TLS to capture upper-level/roof-level data. UAV photogrammetry could be used to make up for the inability of TLS to capture roof data as well as speed up or reduce the scope of a desk study to be conducted, as recommended by Baik et al. [6].

Siwiec and Lenda researched integrating TLS and UAV photogrammetry in 2022 [7]. Their paper studied the application of the combination of TLS and UAV photogrammetry to assess the geometrical properties of industrial chimneys. UAV photogrammetry was used to compensate for the loss of point density from TLS as the distance from the scanning station increased. i.e., TLS accuracy reduces as the height of the chimney increases.

The two data sets were combined using target reference points visible in both data sets. Calibration in this method was limited by the accuracy of the target points recorded by the TLS scan at the higher levels of the chimney. Therefore, the accuracy of integration is reduced. Siwiec and Lenda recommended using ground control points or GPS coordinates, which should increase the accuracy of the integration.

Another paper investigated the integration of TLS and UAV photogrammetry for 3D documentation of a heritage building in Jeddah, Saudi Arabia. This paper utilised an iterative closest point (ICP) algorithm to merge the two data sets. ICP is an algorithm that considers the other data set's nearest point, the linking point. The process is conducted iteratively until a suitable tolerance is reached. The accuracy is limited by the number of iterations allowed. Additionally, the algorithm required images to have high overlap. The angle of view between TLS and UAV photogrammetry scans should fall between 15-20 degrees to maintain accuracy [8].

A study conducted in Jordan in 2019 involved using TLS and digital photogrammetry to optimise the visual quality and geometric data captured from heritage sites. Photogrammetry was used to obtain information on linear and edge surface features, and the model geometric coordinate and scale were obtained from TLS. Combining these two technologies allowed the generation of accurate 3D geometry of the heritage site being investigated. Again, this method is limited by its ability to capture data at higher elevations [9].

Hoon and Hong, in 2019, investigated the integration of TLS and UAV photogrammetry for 3D documentation and spatial analysis of cultural heritage sites in Korea [10]. The integration was achieved by using GCP to merge the two data sets to produce a hybrid point cloud, which was then used to develop a 3D model of heritage site studies. The paper was able to merge the two data sets quite accurately in the x and y axes. There is room for improvement on the z-axis integration. They have also developed a work process for integrating TLS and UAV photogrammetry using GCP to generate a 3D model. Their work process shall be adopted and modified to include GPS coordinating linking for integration and additional steps in generating an HBIM model.

Past works have shown the applicability of both technologies to generate 3D data sets of structures. Some work is being conducted on their combination to produce 3D models of heritage sites. However, an area lacking in research is the combination of both technologies to produce an HBIM model of the heritage sites.

2.1. Terrestrial laser scanning (TLS)

Faro Focus M70 [11] will be used as the laser scanning device for TLS. The Faro Focus M70 has a 3D point accuracy of about 3mm at 10m with a maximum range of 70m. A point spacing of 6mm was used for laser scanning at 10m. It is estimated that each scan will take about 10 - 15 minutes to complete, including acquiring image data. Additionally, the scanner comes with a GNSS system, allowing GPS points to be located within the generated point cloud. The scanner specification meets the requirements for generating an accurate 3D point cloud for generating HBIM models. Target points will be used to register the different scans together. The target points would either be the FARO Checkerboard printed on A4 sheets or the FARO Standard Registration Spheres. These targets provide reference points in the generated scans to allow them to be combined. At least three targets should be visible in each scan. The TLS point cloud shall be processed using FARO Scene, the proprietary software from FARO. Table 1 compares the Focus M70 and the highest specification of the Focus S350 plus.

Table 1. Comparison between the Focus M70 and Focus S350 Plus scanner models.

Item	Focus M70	Focus S350 Plus
Unambiguity Interval	614m for up to 0.5 mil pts/sec	614m for up to 0.5 mil pts/sec 307m for up to 1 mil pts/sec 153m for up to 2 mil pts/sec
Range	0.6 – 70m	0.6 – 350m

Unambiguity interval can be described as the property of phase shift measurements. The value should be higher than the maximum distance to avoid ambiguous measurements. The range represents the maximum scanning distance from the scanner to the scanning objects. In both cases, the M70 is sufficient for this investigation as the scanners will be placed within 10m to 20m of the objects of interest. Eliminating the need for an extensive range and unambiguity interval.

2.2. Unmanned Aerial Vehicle (UAV) photogrammetry

The DJI Phantom 4 Pro V2 will be used for the UAV photogrammetry. This drone has a 20 MP camera featuring a 1" CMOS sensor, a global mechanical shutter, and a GNSS receiver. The images captured automatically store GPS data. The DJI Phantom 4 Pro V2 is well-suited for photogrammetry due to its high-quality camera, low cost, strong image stabilisation, automatic obstacle avoidance, and global mechanical shutter. The global mechanical shutter simultaneously exposes the entire image, reducing distortion during image capture while the UAV is in motion [12]. In contrast, most consumer-grade UAVs use rolling electronic shutters, which cause image distortion as different parts of the image are exposed at different times and locations unless the UAV is completely stationary. While photogrammetry software can correct this distortion to some extent [13], it is preferable to avoid the issue altogether.

For optimal data capture, sufficient image overlap is necessary. In each set of three images, there should be an 80% overlap between the first and second images and a 30% overlap between the first and third images. Additionally, GCP points should be visible in the overlapping images. To effectively combine TLS and UAV

photogrammetry, the viewing angles of the two scans should ideally fall within a range of 15 to 25 degrees [14].

The UAV images will be processed using Global Mapper. Global Mapper was chosen due to the speed of processing. As is common with most image-based modelling software built around Structure from Motion (SfM), images with high overlap and no abrupt angle changes are required to produce data sets of good alignment and scale. The point cloud's absolute datum will be generated by integrating the chosen ground control points or GPS coordinates [13]. Table 2 compares the DJI Phantom 4 Pro V2 and the higher specification model- the Trinity f90+ drone.

Table 2. Comparison between DJI Phantom 4 Pro V2 and Trinity f90+ [15].

	DJI Phantom 4 Pro V2	Trinity f90+
Sensor	CMOS 20 MP	CMOS 42.4 MP
Lens	F2.8	F2.0
Flight Time	30 mins	60 - 90 mins
Flight Mode	Quadcopter	Fixed Wing

Both drones use CMOS sensors, with the Trinity capable of producing much higher quality pictures at 42.4 MP. However, the 20 MP sensor present in the DJI is sufficient to produce detailed point clouds from UAV photogrammetry. Furthermore, both lenses have similar apertures. The flight times of both UAVs are irrelevant as drone scanning is expected to take less than 30 minutes due to the small size of the scanning area. The main deciding factor was the flight modes of the two UAVs. The Trinity is a fixed-wing aircraft that needs a suitable runway for takeoff and to reach its travelling height; it also requires a wide turning angle, making it unsuitable for scanning in an urban area. In our case, the Sarawak Borneo Cultures Museum, a building with a high elevation and close proximity to our scanning area, made the trinity unsuitable. The DJI Phantom 4 Pro V2 allows for vertical takeoff, eliminating the need for a runway and horizontal translation without the need for a large tuning angle. Making it ideal for our case study.

3. Methods

Case studies have been widely adopted as a research method. Case studies are an empirical research method to investigate contemporary phenomena within real-life contexts. They focus on analysing the dynamics of the case being investigated. Case studies are particularly suitable for addressing "how" and "why" research questions when all variables cannot be controlled [16]. This study employs a case study approach to investigate the use of TLS and UAV photogrammetry in developing an HBIM model. The case selected for this investigation is the Sarawak Islamic Heritage Museum.

3.1. Case study: Sarawak Islamic Heritage Museum

The building currently houses the Sarawak Islamic Heritage Museum, built in 1930. It was constructed as a college called James Brooke Malay College, later converted into a school for Islamic studies. The school was called Madrasah Melayu Sarawak. In May 1992, the building was officially officiated as the Sarawak Islamic Heritage

Museum- the first Islamic Heritage Museum in Sarawak, shown in Fig. 2. The museum holds a lot of heritage significance, being a part of the Old Kuching Smart Heritage Trail. The Old Kuching Smart Heritage Trail encompasses various businesses, monuments, and buildings with a significant heritage in Kuching [17].

The building consists of a raised floor and two inner courtyards about 60m long and 40m wide. It houses seven galleries, each with its own story to tell. The galleries cover areas such as the history of Islam in Sarawak and its contributions to science, architecture, and the development of Islam throughout the world. The museum is home to 734 artefacts with high historical/heritage value [17].



Fig. 2. Sarawak Islamic heritage museum.

3.2. Preliminary site investigation

From the preliminary site investigation conducted. It was estimated that about 200 scans were required using the Faro 3D Scanner to cover the entire building, including all architectural features. About 50 scans are required from the exterior and 150 to cover the interior structures. It is estimated that this scanning will take about two weeks to complete. Further to the above, it was noted that about 4 Ground Control Points (GCP) would be sufficient to produce an accurate integration of the TLS and UAV photogrammetry point clouds [18]. The positions of the GCPs were identified during the preliminary site investigation. Furthermore, it was identified that about 100 photographs were required to produce the UAV photogrammetry data set.

3.3. Scan to HBIM workflow

The work process developed is a modified work process developed in 2019 by Hoon, Hong [10], and Elshafey et al. [19]. Modifications include additional steps for developing an HBIM model and integration using GPS coordinates. The overall work process to develop the HBIM model is described in Fig. 3.

The Scan-to-HBIM process involves several stages, starting with data collection using Terrestrial Laser Scanning (TLS) and Unmanned Aerial Vehicle (UAV) photogrammetry. First, data is gathered (levels 1-2) and processed into 3D point clouds (level 3). The point clouds from both methods are then integrated using Ground Control Points (GCPs) or GPS data (level 4) and imported into BIM software (level 5) for developing the HBIM model (level 6).

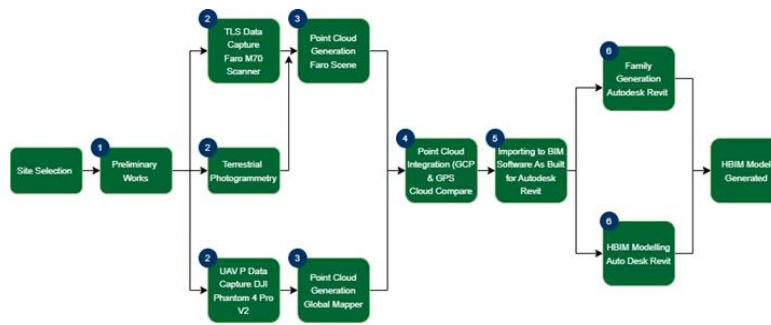


Fig. 3. Modified scan to HBIM workflow [10, 19].

In TLS data processing, scans are registered and combined using target points and georeferenced with GPS data to produce the final point cloud [20]. For UAV photogrammetry, the photos are processed in Global Mapper, using either GCP coordinates or stored GPS data. The images are merged, ensuring at least 80% overlap and 30% side lap, producing an orthophoto model and eventually a point cloud [14].

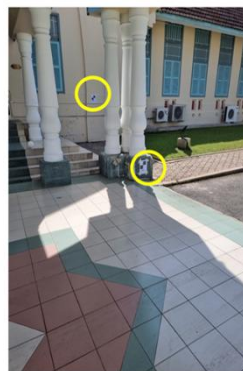
Once both point clouds are generated, they are integrated by aligning common points using Cloud Compare software, which can also create 3D meshes. The integrated 3D model is then imported into Autodesk Revit, where the FARO As-Built plugin helps convert the point cloud into the HBIM model.

3.4. TLS workflow

The TLS (Terrestrial Laser Scanning) process involved scanning both the exterior and interior of the building. For the exterior, 51 scans were performed, while 124 scans were needed for the interior, taking 3 weeks to complete. Faro Spheres and Chequered Boards were used to ensure accurate registration between scans, requiring at least three reference targets to overlap in subsequent scans. A minimum of three reference targets needed to be present in subsequent scans to ensure accurate registration between them. Fig. 4(a) displays the Faro M70 scanner, while Fig. 4(b) illustrates the chequered boards.



(a) Faro M70 scanner.



(b) Chequered boards.

Fig. 4. Faro M70 scanner and chequered boards.

The "Outdoor: 20m" scan profile was used for the exterior, suitable for objects within a 20-meter range. The settings were 1/4 resolution and 4X quality, resulting in a scan time of just over 10 minutes per scan and a point distance of 6.1mm at 10 meters. Interior scans followed the same settings but used the "Interior: 10m" profile, optimised for shorter distances, as shown in Fig. 5.

Once the scans were complete, they were imported into Faro Scene software for processing and manual registration. During registration, two scans were matched by identifying corresponding target markers. When markers were not visible, natural features like drain edges or window corners were used for alignment. The point cloud was optimised using cloud-to-cloud registration. Finally, the project was aligned to a coordinate system using GPS data embedded in the scans. This produced the final point cloud model, ready for further use in the HBIM workflow, as shown in Fig. 6.

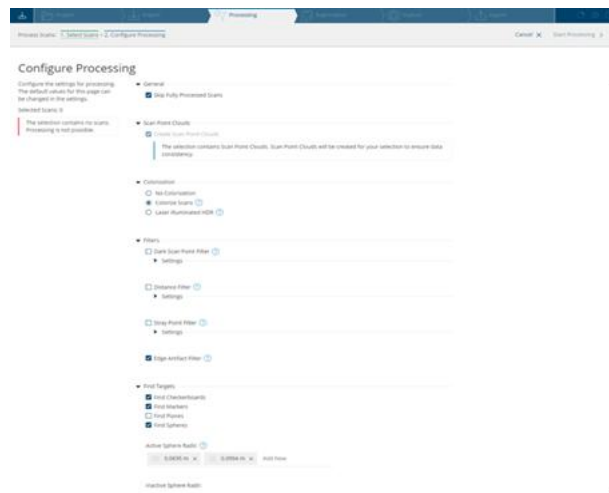


Fig. 5. Faro scene processing setting.

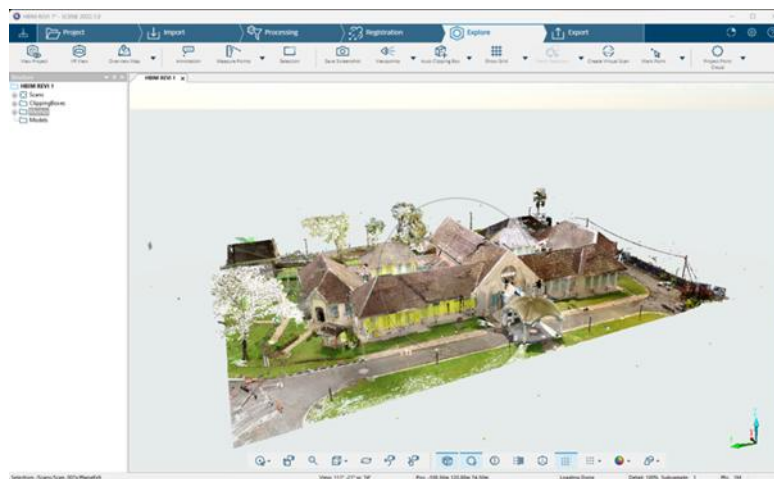


Fig. 6. Final point cloud model for Sarawak Islamic Heritage Museum.

3.5. Unmanned Aerial Vehicle (UAV) photogrammetry workflow

The UAV photogrammetry scan was completed in one day, and a single flight was planned to use DJI Flight Planner software. The drone flew at an altitude of 70 meters and a speed of 3.5 m/s, resulting in a 1.9 cm per pixel resolution. To ensure 80% overlap between images, photos were automatically taken every 2 seconds, capturing 86 images during the flight.

The UAV's camera, Fig. 7(a), with a 3:2 aspect ratio and auto white balance, was set to a -90° nadir orientation for a downward-facing flight plan, as shown in Fig. 7(b). Four ground control points (GCPs) were placed at the edges of the project area to enhance accuracy. These GCPs, made of red-coloured cardboard, were surveyed using RTK technology to ensure precise coordinates. Four GCPs followed recommendations from Zimmerman et al. [21] and Martínez-Carricondo et al. [18], as shown in Fig. 8.

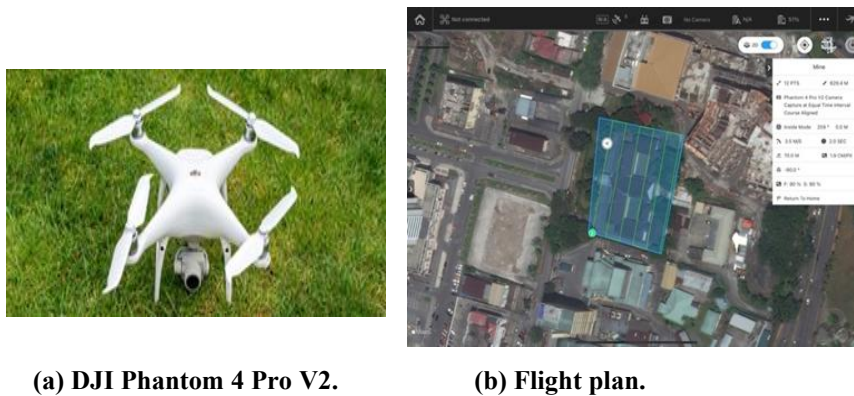


Fig. 7. The DJI Phantom 4 Pro V2 and flight plan.

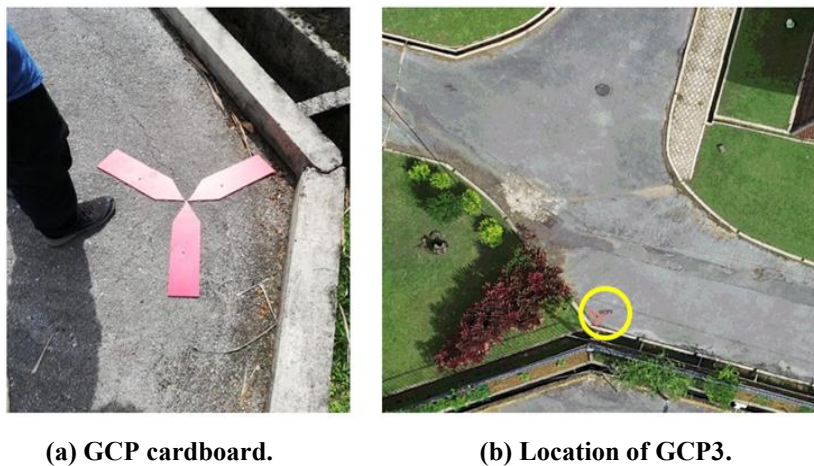


Fig. 8. The four GCPs.

After the flight, the captured images were imported into Global Mapper software. The GPS coordinates embedded in the photos and the GCP coordinates

were used to create a georeferenced image of the project area. The images were then processed into an orthophoto model and transformed into a point cloud, as shown in Fig. 9. Two sets of orthophotos and point clouds were generated: one georeferenced using GCP data and the other using the GPS data from the images. This workflow produced accurate geospatial models for further use in the project.

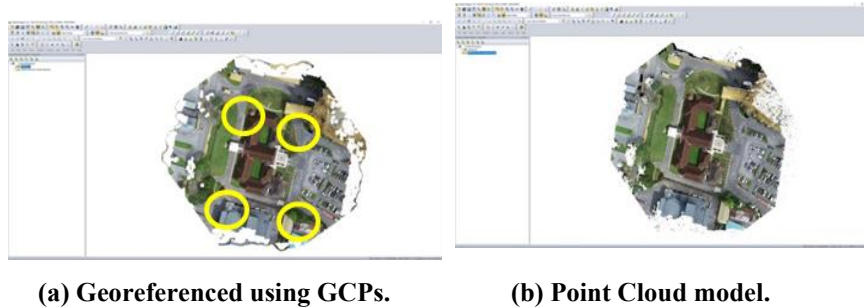


Fig. 9. The processed images.

3.6. TLS and UAV photogrammetry point cloud integration

The point clouds generated from TLS, UAV photogrammetry with GCPs, and UAV photogrammetry with GPS were exported as .e57 files and imported into Cloud Compare software. No further alignment was needed since all point clouds were already georeferenced to the same coordinate system. Using Cloud Compare's "combine point clouds" function, the point clouds were merged, and outlier data points were removed using the segmentation tool. The processed images were shown in Fig. 10(a) and Fig. 10(b).

The combined point clouds (TLS + UAV with GCPs and TLS + UAV with GPS) were exported as .e57 files and converted to .rcp files using Autodesk Recap for import into Revit. This allowed the integrated data to be used for modelling and analysis in Revit.

For family creation in Revit, specific components like windows and doors were isolated using the segmentation tool in Cloud Compare and exported as .pts files, essential for creating accurate Revit families, especially when using the As-Built plugin.

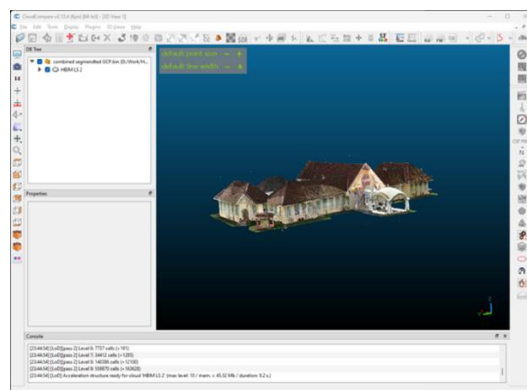


Fig. 10(a). TLS and UAV using point cloud GCP.

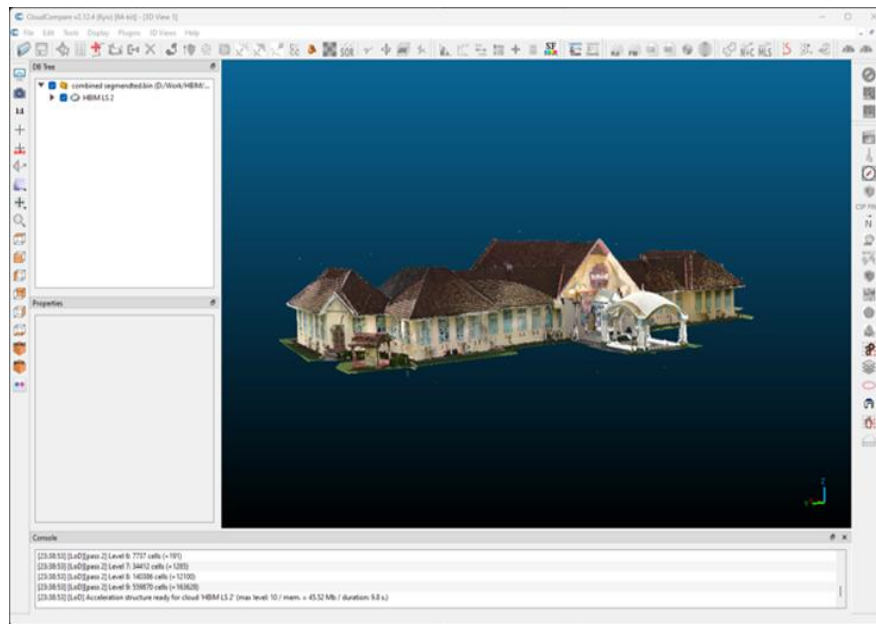


Fig. 10(b). TLS and UAV using point cloud GPS.

3.7. HBIM workflow

This study adopted the scan-to-BIM workflow suggested by Elshafey et al. (2020), focusing on point cloud-to-Revit modelling and family creation, though the family creation process is not discussed here. For point cloud-to-BIM modelling, the point cloud was first imported into Revit using the "insert point cloud" function under the As-Built tab. Levels were then assigned to the project based on the point cloud, as shown in Fig. 11.

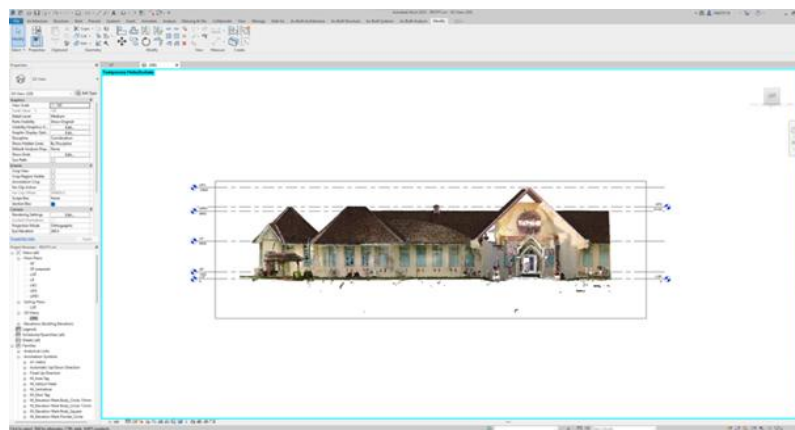


Fig. 11. Assigned levels in the Sarawak Islamic Heritage Museum model.

Next, vertical and horizontal elements like walls were added to the model. Once the walls were in place, windows and doors were inserted using pre-created families.

Floors, artifacts, ceilings, and roofing elements were added afterward, completing the model, as shown in Fig. 12(a).

Figure 12(b) shows the floor plan with all components integrated. This workflow successfully transformed the point cloud data into a detailed 3D model of the building.

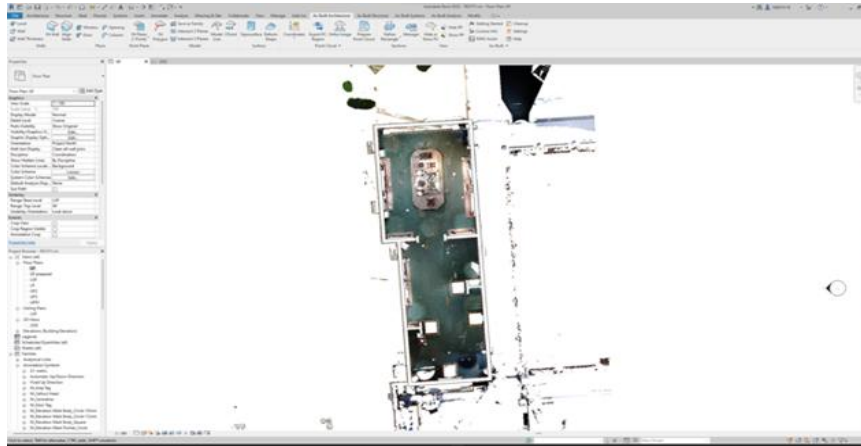


Fig. 12(a). Preliminary model.

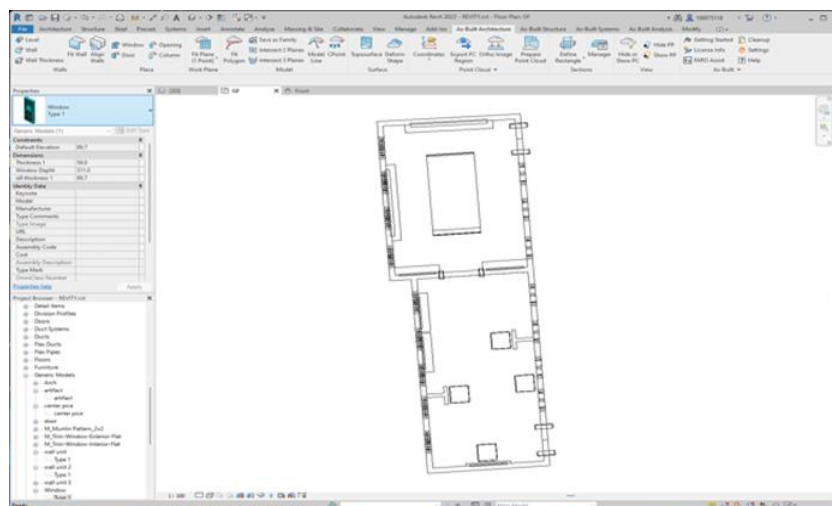


Fig. 12(b). Floor plan for completed model.

4.Results and Discussions

4.1. TLS scan accuracy

To compare different integration techniques, the TLS point cloud is used as the control. Therefore, it is essential to first assess the accuracy of the TLS point cloud itself.

The TLS-generated point cloud showed a mean point error of 2.0 mm, with the maximum error reaching 10.1 mm. Both values fall within the allowed tolerance

set by the Sarawak Building Ordinance 1994 (± 50 mm). This means that, on average, any point in the TLS point cloud is within ± 2 mm of its actual location.

The highest scan overlap recorded was 99.4%, with a mean point error of 0.5 mm, while the lowest overlap was 15.2%, with a mean point error of 1.0 mm. The highest point error (10.1 mm) occurred with an overlap of 46.4%. Figure 13 illustrates the relationship between scan overlap and mean point error. Although there is no strong relationship between overlap and point error, a slight trend of higher overlaps results in lower mean point errors. Even scans with only 26% overlap showed a mean error of 0.6 mm, indicating that the registration process remains accurate regardless of overlap.

Further analysis showed that high mean point errors occurred in three main scenarios. For outdoor scans, errors were higher when sunlight directly hit the scanner's mirror, affecting data recording. These errors were more frequent around noon. Indoor scans showed higher errors when the scanner was placed under bright light or in very dark rooms, while moderate lighting conditions resulted in lower errors.

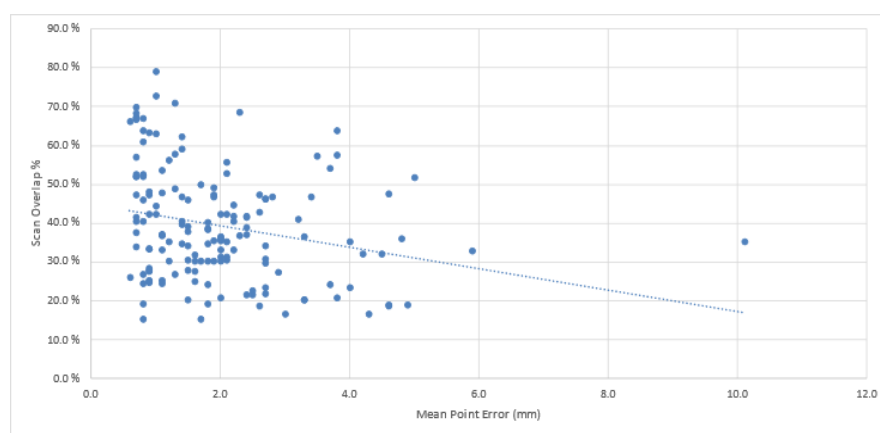


Fig. 13. Relationship between scan overlap and mean point error.

4.2. GCP vs GPS integration

To investigate the accuracy of different integration techniques, the TLS point cloud was used as the control, with two UAV photogrammetry point clouds compared to it. As noted by Wu and Tang [22], TLS can serve as a reliable control for photogrammetry point clouds.

Twenty random points were selected from the TLS point cloud, with ten points on the ground and ten on the building. The distance between the closest UAV photogrammetry points and the corresponding TLS control point was measured. Figure 14 illustrates the points selected for comparison with the UAV photogrammetry point cloud.

The distances between the reference points and the UAV photogrammetry points were measured along the x , y , and z axes. The mean and Root Mean Square (RMS) values were computed and presented in Table 3 for GCP integration and Table 4 for GPS integration. RMS is used to find the absolute deviation of the point clouds from each other, effectively removing the impact of negative values [23].

Accuracy was assessed based on the RMS values, with lower RMS values indicating better integration between the two-point clouds. The comparison data was processed using Cloud Compare software. For GCP integration, the largest difference between the two-point clouds for ground points along the x-axis was 22 mm, with an RMS of 11.53 mm. Along the y-axis, the largest difference was -23 mm, with an RMS of 9.99 mm. For the z-axis, the largest difference was 27 mm, with an RMS of 13.27 mm.

For points on the buildings, the largest difference along the x-axis was -33 mm, with an RMS of 19.81 mm. Along the y-axis, the largest difference was -27 mm, with an RMS of 17.75 mm, and along the z-axis, the largest difference was -30 mm, with an RMS of 21.16 mm.

These results suggest that, on average, points on the TLS point cloud are approximately 11.53 mm, 9.99 mm, and 13.27 mm away from the nearest UAV photogrammetry point in the x, y, and z directions for ground points. For building points, the average distances are 19.81 mm, 17.75 mm, and 21.16 mm in the respective axes.



Fig. 14. Selected reference points.

For GPS integration, as shown in Table 4, the largest differences between point clouds are: 20 mm on the x-axis with an RMS of 13.67 mm, 25 mm on the y-axis with an RMS of 15.80 mm, and -30 mm on the z-axis with an RMS of 18.33 mm for ground points. For building points, the largest differences are -33 mm on the x-axis with an RMS of 22.44 mm, 40 mm on the y-axis with an RMS of 21.20 mm, and 32 mm on the z-axis with an RMS of 23.06 mm. On average, a point in the UAV photogrammetry cloud is about 13.67 mm, 15.80 mm, and 18.33 mm away from the corresponding TLS point for ground points, and 22.44 mm, 21.20 mm, and 23.06 mm away for building points.

Table 3. Accuracy assessment for integration using GCP.

Point	Ground			Building		
	<i>X</i>	<i>Y</i>	<i>Z</i>	<i>X</i>	<i>Y</i>	<i>Z</i>
1	13	12	-2	-13	-20	27
2	13	-5	3	-33	-16	23
3	22	8	-19	20	-1	-11
4	11	-10	-15	21	11	-16
5	-1	4	-2	21	-5	-30
6	-4	5	20	23	23	-19
7	-10	-3	4	0	22	20
8	-11	7	1	24	-19	-15
9	-9	-6	-3	-12	12	-25
10	-8	-23	27	10	-27	18
Mean	1.6	-1.1	1.4	6.1	-10	-2.8
RMS	11.53	9.99	13.27	19.81	17.75	21.16

Table 4. Accuracy assessment for integration using GPS.

Point	Ground			Building		
	<i>X</i>	<i>Y</i>	<i>Z</i>	<i>X</i>	<i>Y</i>	<i>Z</i>
1	20	-15	25	31	-22	32
2	18	-23	-10	22	-13	-25
3	4	5	-19	30	-13	-11
4	-6	11	7	33	31	-11
5	15	-14	-30	15	-21	-21
6	13	-22	-11	10	40	18
7	-11	-6	-18	4	12	15
8	-11	11	-12	6	-2	39
9	-20	25	10	-9	-14	-30
10	7	-11	25	-32	18	4
Mean	2.9	-3.9	-3.3	11	1.6	1
RMS	13.67	15.80	18.33	22.44	21.20	23.06

Based on the results, both integration methods show lower RMS values for ground points than building points, with higher RMS values on the vertical *z*-axis than on the horizontal *x* and *y* axes. The GCP integration method consistently exhibited lower RMS values than GPS integration, indicating superior accuracy.

Both methods meet the tolerance requirements of the Sarawak Building Ordinance 1994 (± 50 mm) and are suitable for building surveying. However, for applications demanding higher precision, GCP integration is preferable. Differences in point cloud accuracy may stem from geometric distortions and shadows affecting UAV photogrammetry, as well as a reduction in point density with distance in TLS scanning, which could explain the higher RMS values for building points.

The accuracy disparity between methods can be attributed to the precision of GCP coordinates versus GPS coordinates. GCPs, obtained through RTK surveys,

offer more accurate data than GPS. While GPS integration provides faster results due to automatic coordinate recording by the drone's sensor, it sacrifices some accuracy. Both integration techniques are effective, but GCP integration delivers greater accuracy, albeit with slightly longer surveying times.

This research underscores the pivotal role of fieldwork in ensuring the effective application of Terrestrial Laser Scanning (TLS) and UAV photogrammetry in developing Heritage Building Information Modelling (HBIM). Key fieldwork activities, such as the strategic placement of Ground Control Points (GCPs) and the implementation of precise data acquisition techniques, significantly impact the overall accuracy and reliability of the generated models. The integrated measurement approach, which combines TLS and UAV photogrammetry, not only capitalises on the strengths of both methods—TLS's detailed geometric accuracy and UAV photogrammetry's extensive coverage—but also mitigates their respective limitations. The proposed workflow highlights the necessity of flexibility in field procedures, particularly in addressing challenges posed by environmental conditions, building geometry, and material properties.

Moreover, this integration holds substantial implications for heritage conservation, enabling the creation of detailed, georeferenced 3D models essential for restoration, digital archiving, and further architectural analysis. This study provides clear guidance for projects where precision is prioritized over speed by demonstrating that GCP-based integration yields superior accuracy compared to GPS-based methods. However, the faster acquisition times associated with GPS-based workflows present advantages in time-sensitive contexts, emphasising the need to tailor the methodology to the project's specific demands. These findings contribute to the foundation for future advancements in multimodal data integration, highlighting the potential for combining emerging technologies, such as AI-driven analysis and high-resolution sensors, to overcome existing limitations in HBIM applications.

5. Conclusion

This paper investigated the accuracy of two integration techniques for combining TLS and UAV photogrammetry point clouds, GCP and GPS, to develop a workflow for creating an HBIM model. Three-point clouds were generated: one from TLS, one from UAV photogrammetry with GCPs, and one from UAV photogrammetry with GPS. The integration of these point clouds was evaluated, revealing that GCP integration achieved higher accuracy (lower RMS values) compared to GPS integration. Both methods demonstrated higher accuracy for ground points than building points, but all results fell within the tolerance limits of the Sarawak Building Ordinance 1994, making them suitable for building surveys. GPS integration offered faster processing, whereas GCP integration provided better accuracy, making the choice dependent on the need for precision or speed.

The paper also proposed a detailed workflow for using TLS and UAV photogrammetry to produce an HBIM model. This workflow included preliminary site work, data collection, point cloud processing, integration, family modelling, and HBIM modelling. The proposed process successfully created an HBIM model of the Second Gallery (Islamic Architecture) of the Islamic Heritage Museum Sarawak.

This research faced several limitations related to the chosen equipment's data capture capabilities and the scanning process's nature. While the equipment used

was sufficient for the study, more advanced tools like the FARO Focus S360 could offer better data quality and accuracy. Material properties posed another challenge, as reflective surfaces like glass can distort laser measurements, affecting the accuracy of TLS scans. Additionally, TLS scanning cannot detect hidden elements like mechanical and electrical fixtures within walls or floors nor scan spaces between ceilings and roofs. Despite these challenges, the research successfully demonstrated the integration of various data capture techniques for building surveys. Future research with more advanced technologies could overcome these limitations and achieve even more precise and comprehensive results.

References

1. Osello, A.; and Rinaudo, F. (2016). *Cultural heritage management tools: The role of GIS and BIM*. In Stylianidis E.; and Remondino, F. (Eds.), *3D Recording, Documentation and Management of Cultural Heritage*. Whittles Publishing.
2. Zhang, J.; and Lin, X. (2017). Advances in the fusion of optical imagery and LiDAR point cloud applied to photogrammetry and remote sensing. *International Journal of Image and Data Fusion*, 8(1), 1-31.
3. Lenda, G.; Marmol, U.; and Mirek, G. (2015). Accuracy of laser scanners for measuring surfaces made of synthetic materials. *Photogrammetrie - Fernerkundung - Geoinformation*, 5, 357-372.
4. Karachaliou, E.; Georgiou, E.; Psaltis, D.; and Stylianidis, E. (2019). UAV for mapping historic buildings: From 3D modelling to BIM. *ISPRS Annals of the Photogrammetry, Remote Sensing and Spatial Information Sciences*, 42, 397-402.
5. Ioannides, M.; Fritsch, D.; Leissner, J.; Davies, R.; Remondino, F.; and Caffo, R. (2012). *Progress in cultural heritage preservation: 4th international conference, EuroMed 2012, Limassol, Cyprus, October 29 - November 3, 2012. Proceedings*. Springer Berlin Heidelberg, 76-85.
6. Baik, A.; Almainani, A.; Al-Amadi, M.; and Rahaman, K.R. (2021). Applying digital methods for documenting heritage building in Old Jeddah: A case study of Hazzazi House. *Digital Applications in Archaeology and Cultural Heritage*, 21, 1-15.
7. Siwiec, J.; and Lenda, G. (2022). Integration of terrestrial laser scanning and structure from motion for the assessment of industrial chimney geometry. *Measurement*, 199, 111404.
8. Baik, A. (2017). From point cloud to Jeddah Heritage BIM Nasif Historical House-case study. *Digital Applications in Archaeology and Cultural Heritage*, 4, 1-18.
9. Alshawabkeh, Y.; El-Khalili, M.; Almasri, E.; Bala'awi, F.; and Al-Massarweh, A. (2020). Heritage documentation using laser scanner and photogrammetry. The case study of Qasr Al-Abidit, Jordan. *Digital Applications in Archaeology and Cultural Heritage*, 16, 1-6.
10. Hoon, Y.J.; and Hong, S. (2019). Three-dimensional digital documentation of cultural heritage sites based on the convergence of terrestrial laser scanning and unmanned aerial vehicle photogrammetry. *ISPRS International Journal of Geo-Information*, 8, 53.

11. Faro. (2022). Technical specification sheet for the focus laser scanner. FARO® knowledge base. Retrieved February 14, 2023, from https://knowledge.faro.com/Hardware/Focus/Focus/Technical_Specification_Sheet_for_the_Focus_Laser_Scanner
12. Vautherin, J. et al. (2016). Photogrammetric accuracy and modeling of rolling shutter cameras. *ISPRS Annals of the Photogrammetry, Remote Sensing and Spatial Information Sciences*, 3, 139-146.
13. Zhou, Y.; Daakir, M.; Rupnik, E.; and Pierrot-Deseilligny, M. (2020). A two-step approach for the correction of rolling shutter distortion in UAV photogrammetry. *ISPRS Journal of Photogrammetry and Remote Sensing*, 160, 51-66.
14. Martínez-Carricondo, P.; Carvajal-Ramírez, F.; Yero-Paneque, L.; and Agüera-Vega, F. (2021). Combination of HBIM and UAV photogrammetry for modelling and documentation of forgotten heritage. Case study: Isabel II dam in Níjar (Almería, Spain). *Heritage Science*, 9, 95.
15. Themes Boss. (2023). Drone nerds: DJI, HLCM Group. Retrieved February 14, 2023, from <https://www.hlcmgroup.com/drones-sensors.php>
16. Teegavarapu, S.; Summers, J.D.; and Mocko, G.M. (2008). Case study method for design research: A justification. *Proceedings of the ASME 2008 International Design Engineering Technical Conferences and Computers and Information in Engineering Conference*, Brooklyn, New York, USA, 495-503.
17. Sarawak Museum Department. (2023). Retrieved February 14, 2023, from https://museum.sarawak.gov.my/web/subpage/announcement_list/
18. Martínez-Carricondo, P.; Agüera-Vega, F.; Carvajal-Ramírez, F.; Mesas-Carrascosa, F-J.; García-Ferrer, A.; and Pérez-Porras, F-J. (2018). Assessment of UAV-photogrammetric mapping accuracy based on variation of ground control points. *International Journal of Applied Earth Observation and Geoinformation*, 72, 1-10.
19. Elshafey, A.; Chai C.S.; Eeydzah, A.; Gheisari, M.; and Usmani, A. (2020). Technology acceptance model for Augmented Reality and Building Information Modeling integration in the construction industry. *Journal of Information Technology in Construction*, 25, 161-172.
20. Pavelka, K. (2022). Photogrammetry, laser scanning and HBIM for construction diagnostic. *The International Archives of the Photogrammetry, Remote Sensing and Spatial Information Sciences*, 46, 171-176.
21. Zimmerman, T.; Jansen, K.; and Miller, J. (2020). Analysis of UAS flight altitude and ground control point parameters on DEM accuracy along a complex, developed coastline. *Remote Sensing*, 12(14), 2305.
22. Wu, B.; and Tang, S. (2015). Review of geometric fusion of remote sensing imagery and laser scanning data. *International Journal of Image and Data Fusion*, 6(2), 97-114.
23. Ulvi, A. (2021). Documentation, Three-Dimensional (3D) modelling and visualization of cultural heritage by using Unmanned Aerial Vehicle (UAV) photogrammetry and terrestrial laser scanners. *International Journal of Remote Sensing*, 42(6), 1994-2021.